1521-0111/92/2/101–112$25.00
MOLECULAR PHARMACOLOGY

https://doi.org/10.1124/mol.116.107797
Mol Pharmacol 92:101–112, August 2017

α2 Subunit–Containing $GABA_A$ Receptor Subtypes Are Upregulated and Contribute to Alcohol-Induced Functional Plasticity in the Rat Hippocampus

A. Kerstin Lindemeyer, Yi Shen, Ferin Yazdani, Xuesi M. Shao, Igor Spigelman, Daryl L. Davies, Richard W. Olsen, and Jing Liang

Department of Molecular and Medical Pharmacology (A.K.L., Y.S., F.Y., R.W.O., J.L.), and Department of Neurobiology (X.M.S.), David Geffen School of Medicine at University of California at Los Angeles, and Division of Oral Biology and Medicine, School of Dentistry (I.S.), University of California and Titus Family Department of Clinical Pharmacy, University of Southern California School of Pharmacy (D.L.D., J.L.), Los Angeles, California

Received December 13, 2016; accepted May 5, 2017

ABSTRACT

Alcohol (EtOH) intoxication causes changes in the rodent brain γ-aminobutyric acid receptor ($GABA_AR$) subunit composition and function, playing a crucial role in EtOH withdrawal symptoms and dependence. Building evidence indicates that withdrawal from acute EtOH and chronic intermittent EtOH (CIE) results in decreased EtOH-enhanced $GABA_AR$ δ subunit-containing extrasynaptic and EtOH-insensitive $\alpha1\beta\gamma2$ subtype synaptic $GABA_ARs$ but increased synaptic $\alpha4\beta\gamma2$ subtype, and increased EtOH sensitivity of $GABA_AR$ miniature postsynaptic currents (mIPSCs) correlated with EtOH dependence. Here we demonstrate that after acute EtOH intoxication and CIE, upregulation of hippocampal $\alpha4\beta\gamma2$ subtypes, as well as increased cell-surface levels of $GABA_AR$ $\alpha2$ and $\gamma1$ subunits, along with increased $\alpha2\beta1\gamma1$ $GABA_AR$ pentamers in hippocampal slices using cell-surface cross-linking, followed by Western blot and coimmunoprecipitation. One-dose and two-dose acute EtOH treatments produced temporal plastic changes in EtOH-induced anxiolysis or withdrawal anxiety, and the presence or absence of EtOH-sensitive synaptic currents correlated with cell surface peptide levels of both $\alpha4$ and $\gamma1$(new $\alpha2$) subunits. CIE increased the abundance of novel mIPSC patterns differing in activation/deactivation kinetics, charge transfer, and sensitivity to EtOH. The different mIPSC patterns in CIE could be correlated with upregulated highly EtOH-sensitive $\alpha2\beta\gamma$ subtypes and EtOH-sensitive $\alpha4\beta\gamma2$ subtypes. Naïve $\alpha4$ subunit knockout mice express EtOH-sensitive mIPSCs in hippocampal slices, correlating with upregulated $GABA_AR$ $\alpha2$ (and not $\alpha4$) subunits. Consistent with $\alpha2$, $\beta1$, and $\gamma1$ subunits genetically linked to alcoholism in humans, our findings indicate that these new $\alpha2$-containing synaptic $GABA_ARs$ could mediate the maintained anxiolytic response to EtOH in dependent individuals, rat or human, contributing to elevated EtOH consumption.

Introduction

γ-Aminobutyric acid type A receptors ($GABA_ARs$) are major targets of ethanol (EtOH) action in the brain. $GABA_ARs$ are heteromeric chloride channels of the Cys-loop pentameric ligand-gated ion channel family that mediate most of the inhibitory neurotransmission in the mammalian central nervous system. More than 20 $GABA_AR$ subunit combinations have been identified, derived from a family of 19 subunit genes divided into eight classes according to sequence homology: α1-6, β1-3, γ1-3, δ, ε, θ, π, and ρ1-3 (Olsen and Sieghart, 2008), many found organized in clusters on human chromosomes 4 ($\alpha4$, $\beta1$, $\alpha2$, $\gamma1$), 5 ($\alpha6$, $\beta2$, $\alpha1$, $\gamma2$), 15 ($\beta3$, $\alpha5$, $\gamma3$), and X (θ, $\alpha3$, ε) (McLean et al., 1995; Simon et al., 2004). In the forebrain, typically, 2α and 2β are present with either one γ or one δ subunit in each pentamer.

According to the subunits present, distinct $GABA_ARs$ have different pharmacology, channel kinetics, and topography, with resulting functional and behavioral consequences (Puia et al., 1991; Whiting et al., 1999; Olsen and Sieghart, 2008). Primarily in combination with $\alpha2$ or $\alpha1$, $\gamma2$-containing subtypes cluster to a greater extent at postsynaptic sites, interacting with the inhibitory postsynaptic scaffold protein gephyrin (Essrich et al., 1998). The presence of the δ subunit confers extrasynaptic localization (Nusser et al., 1998), producing EtOH sensitivity of the tonic inhibitory current (I_{tonic}). We and others have shown that low millimolar EtOH enhances δ-$GABA_AR$ tonic inhibition in neurons (Hanchar et al., 2005; Liang et al., 2006; Mody et al., 2007) and in recombinant systems (Sundstrom-Poromaa et al., 2002; Wallner et al., 2003). This EtOH enhancement in slices is interpreted by some as indirect action on GABA release (Borghese et al., 2006; Weiner and Valenzuela, 2006; Lovinger

This work was supported by the United States Public Health Service grants to R.W.O. [Grants AA007680 and AA021213], to J.L. [Grant AA017991], and to I.S. [Grants AA016100 and AA022408].
https://doi.org/10.1124/mol.116.107797.

ABBREVIATIONS: ACSF, artificial cerebrospinal fluid; CIE, chronic intermittent ethanol; CIV, chronic intermittent vehicle; co-IP, coimmunoprecipitation; DG, dentate gyrus; DGC, dentate gyrus granule cell; EPM, elevated plus maze; EtOH, ethanol; GABA, γ-aminobutyric acid; $GABA_AR$, γ-aminobutyric acid type A receptor (ionotropic); MANOVA, multivariate analysis of variance; mIPSC, miniature inhibitory postsynaptic current; WT, wild-type.

and Homanics, 2007). $GABA_A$Rs and their EtOH-induced plastic changes have long been implicated in EtOH's acute effects and dependence (Follesa et al., 2004; Kumar et al., 2009; Olsen and Spigelman, 2012). Moreover, chronic intermittent ethanol (CIE) administration to rodents produces long-lasting alterations in hippocampal $GABA_A$R subunit expression at cell surfaces and corresponding changes in $GABA_A$R-mediated inhibitory synaptic and extrasynaptic tonic currents, pharmacology, and behavior (Cagetti et al., 2003; Liang et al., 2004, 2006). CIE administration results in a persistent decrease of $\alpha1$ and δ and increased $\alpha4$ and $\gamma2$ subunits. The observed net subunit switch ($\alpha1$ to $\alpha4$ and δ to $\gamma2$) suggests a decrease of mostly $\alpha1\beta\gamma2$ (synaptic) and $\alpha4\beta\delta$ (extrasynaptic) $GABA_A$Rs and an increase of $\alpha4\beta\gamma2$ $GABA_A$Rs, including $\alpha4$ appearing at central locations of symmetric synapses. I_{tonic} and its enhancement by EtOH are reduced, but the miniature inhibitory postsynaptic currents (mIPSCs) become sensitive to enhancement by EtOH (Liang et al., 2006). Accompanying behavioral alterations are consistent with alcohol dependence, including increased anxiety and seizure susceptibility and tolerance to the sedative-hypnotic, but not anxiolytic, effects of EtOH and other GABAergic modulatory sleep aids (Liang et al., 2009; Olsen and Spigelman, 2012). Rats administered intermittent regimens of EtOH have demonstrated increased EtOH preference in voluntary consumption assays (Rimondini et al., 2003; O'Dell et al., 2004; Simms et al., 2008). Similar, but transient, hippocampal changes in $GABA_A$R subunits and inhibitory currents can be observed immediately ($\alpha4\beta\delta$-receptor downregulation after 1 hour), continuing to 48 hours (delayed downregulation of $\alpha1\beta\gamma2$-reptors and upregulation of $\alpha4\beta\gamma2$-receptors) after one large dose of EtOH in vivo (Liang et al., 2007; Gonzalez et al., 2012). The $GABA_A$R $\alpha4$ subunit is upregulated in numerous hyperexcitability animal models involving drug withdrawal and/or epilepsy (Schwarzer et al., 1997; Smith and Gong, 2005; Lagrange et al., 2007; Olsen and Spigelman, 2012).

After acute EtOH intoxication and CIE, we investigated: 1) possible increased partnerships between $GABA_A$R $\alpha4$ and $\gamma2$ subunits and whether other subtypes were altered and 2) which $GABA_A$Rs mediate EtOH-sensitive mIPSCs in hippocampal slices from EtOH-treated rats. Previously, recombinant $GABA_A$Rs with differing α subunits and native $GABA_A$Rs in cells with dominant expression of specific α subunits have been distinguished on the basis of activation and inactivation rates, τ, in the order $\alpha4 < \alpha1 < \alpha2$, and $\gamma2 < \gamma1$ (Lavoie et al., 1997; McClellan and Twyman, 1999; Smith and Gong, 2005; Liang et al., 2006; Dixon et al., 2014). We performed coimmunoprecipitation experiments to determine which $GABA_A$R subtypes were altered after EtOH intoxication. We then investigated the time course of plastic changes in EtOH-sensitive mIPSCs relative to subunit and behavioral changes by examining mIPSC recordings using new software for spontaneous synaptic current pattern recognition analysis. We interpret the EtOH-induced, upregulated, EtOH-sensitive $GABA_A$Rs as likely candidates for a role in the anxiolytic response to EtOH, increased EtOH drinking in the dependent individual, and development of dependence.

Materials and Methods

Animals. All protocols followed National Institutes of Health guidelines and were approved by the University of California Institutional Animal Care and Use Committee. Male Sprague-Dawley rats (Harlan/Envigo, www.envigo.com), 200–250 g, were housed in the vivarium under a 12-hour light/dark cycle and had free access to food and water. The $\alpha4$ knockout and wild-type (WT) littermate control mice were produced from heterozygous breeding pairs on a C57BL/6J N7 genetic background at the University of California Los Angeles in an Association for Assessment and Accreditation of Laboratory Animal Care–approved facility. Mouse production and genotyping have been previously reported (Chandra et al., 2006). Only adult male (3 to 4 months old) mice were used in the experiments.

EtOH Treatment. To study acute EtOH effects, rats were administered a single dose of EtOH by gavage (5 g/kg of body weight), as a 25% (w/v) solution in water (Pharmco Products, Brookfield, CT). Control rats were underwent gavage with drinking water (20 ml/kg of body weight). For CIE treatment, rats underwent gavage with 5 g/kg, 25% (w/v) EtOH for the first five doses once every other day, followed by 55 doses of 6 g/kg EtOH 30%, once daily. This CIE paradigm led rats to experience multiple cycles of intoxication and withdrawal. Chronic intermittent vehicle (CIV) rats, as controls, underwent gavage with drinking water (20 ml/kg of body weight) in parallel (Liang et al., 2006). Rats were euthanized (1–48 hours after acute treatment or 40–60 days after CIV or CIE treatment, if not stated otherwise).

Measurement of Surface Receptor Subunit Expression by Cross-Linking. To measure cell surface protein levels of slices from in vivo treated rats, cross-linking experiments followed by Western blot analysis were performed, as described previously (Grosshans et al., 2002). Briefly, 400-μm-thick coronal hippocampal slices were prepared using a vibrating blade microtome (VT1200S; Leica Microsystems, Bannockburn, IL), and the dentate gyrus (DG) and CA1 regions were microdissected. Slices were incubated either in ice-cold artificial cerebrospinal fluid (ACSF) composed of 124 mM NaCl, 3 mM KCl, 1 mM $MgCl_2$, 2 mM $CaCl_2$, 1 mM KH_2PO_4, 10 mM D-glucose, 26 mM $NaHCO_3$, and oxygenated with 95%O_2/5% CO_2, pH 7.4) or ACSF containing 1 mg/ml bis(sulfosuccinimidyl)suberate (BS^3) (Pierce, Rockford, IL) at 4°C for 45 minutes. The cell-impermeable BS^3 bifunctionally cross-links all surface proteins, leading to large-molecular-weight aggregates that do not reliably migrate in the gel. Therefore, only internal proteins show up in the gel of the BS^3 sample. The cross-link reaction was quenched with 20 mM Tris wash buffer, pH 7.6, and the slices were homogenized in homogenizing buffer containing 10 mM Tris, pH 8.0, 1 mM EDTA, and 1% SDS. Protein concentrations were determined using the BCA Protein Assay Kit (Pierce).

Coimmunoprecipitation. Crude membrane proteins were obtained from freshly isolated DG and CA1 hippocampal regions. The tissue was homogenized at 4°C in homogenizing buffer containing 10 mM HEPES, pH 7.5, 1 mM EDTA, 300 mM sucrose, complete protease inhibitor (Roche, Basel, Switzerland), 0.5 mM PMSF, 5 mM sodium fluoride, and 5 mM sodium orthovanadate. The homogenate was centrifuged at 1000*g* for 10 minutes at 4°C to remove pelleted nuclear fraction. To obtain crude membrane fraction, the supernatant was centrifuged at 100,000*g* at 4°C for 30 minutes, and the pellet was resuspended in solubilization buffer containing 50 mM Tris, pH 8.0, 50 mM KCl, 1 mM EDTA, complete protease inhibitor (Roche), 0.5 mM PMSF, 5 mM sodium fluoride, 5 mM sodium orthovanadate, 1.0% Triton X-100, and 0.1% SDS for 30 minutes and was then cleared by ultracentrifugation (100,000*g* at 4°C for 30 minutes). Solubilized proteins were incubated with 10 μg of the respective antibody (see following discussion) for 1 hour at 4°C. Then 50 μl of protein G agarose (Sigma) was added overnight at 4°C. Precipitate was washed with washing buffer containing 20 mM Tris, pH 8.0, and 15% solubilization buffer. Precipitated proteins were eluted with Laemmli sample buffer (Bio-Rad). β-Mercaptoethanol was added after elution. A negative control with 10 μg of normal rabbit IgG (Cell Signaling Technology, Danvers, MA) was performed in parallel for each experiment. For detection of low-affinity or transient bound interaction partners, slices were incubated in ACSF containing 2.5 mM 3,3′-dithiobis(sulfosuccinimidylpropionate) (Pierce), and 3 mM dithiobis(succinimidylpropionate) (Pierce) for 2 hours at 4°C to reversibly cross-link extracellular and intracellular proteins, respectively, before to cell lysis and coimmunoprecipitation (co-IP). The reaction was quenched with 50 mM Tris, pH 7.6, for 30 minutes at 4°C.

To reverse cross-linking, samples were boiled in 5% β-mercaptoethanol in SDS-PAGE sample buffer (Bio Rad) for 5 minutes at 95°C.

SDS-PAGE and Western Blot Analysis. Proteins were separated on SDS-PAGE gels (Bio-Rad, Hercules, CA) using the Bio-Rad Mini-Protean 3 cell system. Proteins were transferred on a polyvinylidene difluoride membrane (Bio-Rad) and blocked with 4% nonfat dry milk in TTBS. Blots were incubated overnight at 4°C with primary polyclonal rabbit antibodies against the following: α1 (NB 300-207; 1:1000; Novus Biologicals, Littleton, CO), α3 (1:500; Abcam, 72446), α2 (aa 416–424) (Zezula et al., 1991) [α2 (aa322–357) (Pöltl et al., 2003) was used for co-IP], α4 (aa379–421) (Ebert et al., 1996), α5 (aa 337–380) (Pöltl et al., 2003), β1 (aa 350–404), β2 (aa 351–405) (Jechlinger et al., 1998), β3 (aa345–408) (Slany et al., 1995), γ1 (aa 1–39) (Pöltl et al., 2003), γ2 (aa 319–366) (Tretter et al., 1997), δ (aa 1–44) (Jones et al., 1997) (all at 1 μg/ml, gift from W. Sieghart); gephyrin (TXsc-14003, 1:500; Santa Cruz, Dallas, TX), or mouse monoclonal β-actin (A2228; 1:1000; Sigma), followed by horseradish peroxidase–conjugated secondary antibodies (1:5000, Rockland Antibodies & Assays, Limerick, PA) or Clean-Blot IP Detection Reagent (Thermo Scientific, Somerset, NJ) for 2 hours at room temperature. Bands were detected using ECL detection kit (Amersham Pharmacia UK, Littlefont, UK) and exposed to X-ray films (MidSci, St. Louis, MO).

Electrophysiological Recordings. Whole-cell patch-clamp recordings were obtained from neurons located in the dentate granule cell layer in transverse slices (400 μm thick) of dorsal hippocampus from rats or mice. The slices were perfused with ACSF (34 ± 0.5°C) equilibrated with carbogen of 95% O_2/5% CO_2 to ensure adequate oxygenation of slices and a pH of 7.4. Patch pipettes were filled with solution containing (in mM) 135 cesium gluconate (or 135 CsCl), 2 $MgCl_2$, 1 $CaCl_2$, 11 EGTA, 10 HEPES, 2 ATP-Na_2, and 0.2 GTP-Na_2, pH adjusted to 7.25 with CsOH. GABA$_A$R-mediated mIPSCs were pharmacologically isolated by adding tetrodotoxin (0.5 μM), D-(−)-2-amino-5-phosphonopentanoate (40 μM), 6-cyano-7-nitroquinoxaline-2,3-dione (10 μM), and CGP 54626 (1 μM) to the ACSF. Whole-cell currents were recorded (voltage clamp at 0 mV or −70 mV) with an amplifier (Axoclamp 2B; Molecular Devices, Union City, CA). Whole-cell access resistances were in the range of 10–25 MΩ and electrically compensated by ~70%. During voltage-clamp recordings, access resistance was monitored by measuring the size of the capacitative transient in response to a 5-mV step command. Intracellular signals were low-pass-filtered at 3 kHz (Axoclamp 2B) and digitized at 20 kHz with Digidata 1200 and software Clampex (Molecular Devices).

Detection and General Analysis of mIPSCs and GABA$_A$R-Mediated I_{tonic}. mIPSCs were detected with amplitude and area threshold criteria using MiniAnalysis Program (version 6.0.7; Synaptosoft Inc. Fort Lee, NJ). The frequency of mIPSCs was determined from all automatically detected events in a given 100-second recording period. For kinetic analysis, only single-event mIPSCs with a stable baseline, sharp rising phase, and exponential decay were used. mIPSCs were scaled averaged and aligned with half rise time. Decay time constants were obtained by fitting exponentials to the falling phase of the averaged mIPSCs. The GABA$_A$R-mediated I_{tonic} magnitudes were obtained as the difference between the averaged baseline current of a given recording period minus the averaged baseline current in the presence of picrotoxin (100 μM, a GABA$_A$R antagonist).

The mIPSC Pattern Recognition Analysis Method. An optimally scaled template algorithm (Clements and Bekkers, 1997) is implemented in DataView software (V9.3, WJ Heitler, University of St Andrews, St Andrews, Scotland). This method finds synaptic events of particular waveforms (shapes) within data trace records. We define a search template by taking an example of the desired mIPSC pattern from a current trace record or taking the average of similar mIPSCs. An acceptable error level is set, which is the degree of similarity an event must have to the templates to be included in the search results. The program searches through the record for similar waveform patterns. During the search, the software scales and offsets the template to find the best match in shape, but not necessarily in size or threshold, and then accepts the match if it falls within the specified error tolerance. We performed pattern recognition (classification) on several data files with a given template.

Anxiety Assay. Anxiety associated with EtOH treatment was measured on an elevated plus maze (EPM) with four arms of 51-cm-long, 11.5-cm-wide arranged at right angles (Liang et al., 2004). Briefly, each animal was placed in the center of the maze facing an open arm and allowed to explore for 5 minutes. During this 5-minute test session, the animal's behavior was recorded on a camcorder. Numbers of arm entries and time spent in each arm per entry were analyzed. An increase in time (%) spent in the closed arms (time in open arms/total time in open and closed arms) in EPM indicates an enhanced anxiety level.

Data Analysis. Biochemistry protein signals were analyzed by densitometry using ImageQuant5.2 (Molecular Dynamics). For cross-linking experiments, the signal intensity of bands was normalized to the corresponding β-actin signal after background subtraction. Surface protein levels were calculated by subtraction of the internal protein signal from the respective total protein signal. Signals for co-IPs were calculated as percentage protein co-IP/protein IP. Sets of control and treatment experiments were always performed in parallel and run on the same gel. Subunit data were analyzed with multivariate analysis of variance (MANOVA) using Proc GLM of SAS program (V9.4; SAS Institute, Cary, NC). Wilks' λ value and its P value for every MANOVA family are reported. P values for comparison of treatment versus control groups were also calculated within MANOVA model. GABAergic currents recorded by whole-cell patch-clamp, behavioral data and subunit measurements for multiple time points were analyzed with one-way or two-way ANOVA, followed by post hoc multiple comparison based on Dunnett's method to determine significant levels between treatments and single controls or Holm-Sidak's method to determine significant levels among groups (pairwise) using SigmaStat (Systat Software Inc. San Jose, CA) or SAS (details in figure legends). $P < 0.05$ was considered statistically significant. All values are shown as mean ± S.E.M., with n representing the number of experiments using different sets of animals.

Results

EtOH Treatment of Rats Induces a Net Switch of GABA$_A$R Subtypes in the Hippocampal Formation. First, changes in cell-surface expression of α1, α4, δ, and γ2 GABA$_A$R subunits were measured 24 hours after rats were administered a single intoxicating dose of EtOH (EtOH 24 hours: 5 g/kg via gavage) using cross-linking experiments on microdissected slices of the DG (Fig. 1, A and B). Compared with vehicle-treated controls, surface α1 levels were decreased to 54.8% ± 8.7% ($n = 5$) in DG. In contrast, the surface levels of the GABA$_A$R α4 subunit in DG were increased to 214.6% ± 16.8% ($n = 5$) compared with vehicle-treated controls (Fig. 1, A and B). Surface δ subunit expression in DG was reduced to 61.4% ± 6.4% ($n = 5$), whereas surface γ2 was increased to 246.1% ± 47.4% ($n = 5$) of control (Fig. 1, A and B). Next, we investigated α1 and α4 surface expression in the CA1 hippocampal region 24 hours after EtOH administration (Fig. 1C). Compared with vehicle-treated rats, we found a decrease in the α1 subunit to 46.6% ± 7.6% ($n = 5$) and an increase in α4 to 188.4% ± 28.6% ($n = 5$) in CA1 (Fig. 1C). Surface expression of the δ subunit was decreased to 70.7% ± 3.3% ($n = 5$), and the γ2 subunit on the cell surface showed a 238.2% ± 25.5% ($n = 5$) increase in the CA1 (Fig. 1 C). These observations are consistent with what has been observed 48 hours after EtOH intoxication and ≥40 days after CIE treatment in CA1 and DG slices (Liang et al., 2007). They also agree with previous studies on cultured hippocampal neurons, where similar plastic changes in GABA$_A$R subunit surface levels were reported 24 hours after EtOH exposure (Shen et al., 2011).

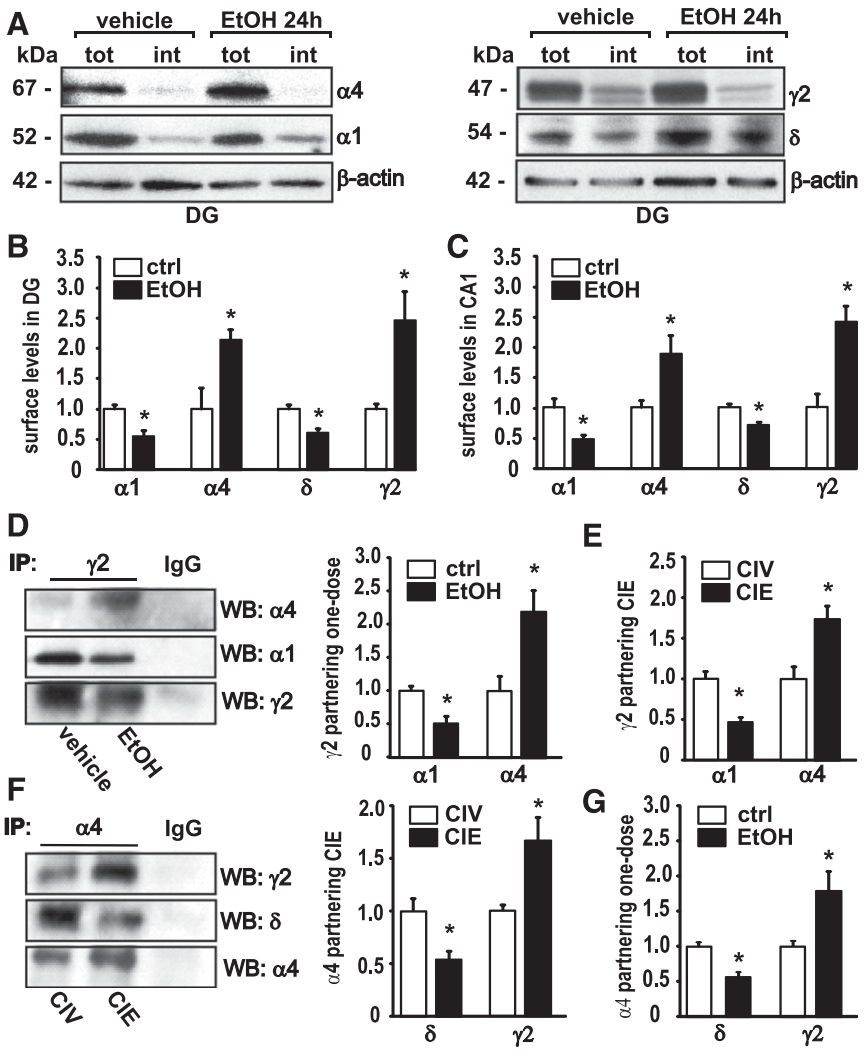

Fig. 1. Acute and chronic EtOH treatments induce a long-term increase in the amount of $\alpha4\gamma2$-containing $GABA_AR$s and a decrease in $\alpha1\gamma2$- and $\alpha4\delta$-containing $GABA_AR$s in rat CA1 + DG. (A) Representative Western blots after cell-surface cross-linking show changes in $GABA_AR$ $\alpha1$ and $\alpha4$ (same blot), left, and in δ and $\gamma2$ subunits (same blot), right. (B) Quantification of the surface levels of $\alpha1$, $\alpha4$, δ, and $\gamma2$ in the DG 24 hours after EtOH intoxication compared with their controls (ctrl). MANOVA analysis, Wilks' $\lambda = 0.0295$, $P = 0.0005$, $n = 5$. (C) Quantification of the surface levels of $\alpha1$, $\alpha4$, δ, and $\gamma2$ in the CA1 24 hours after EtOH intoxication compared with their controls. MANOVA, Wilks' $\lambda = 0.0635$, $P = 0.0034$, $n = 5$. tot, amount of total protein; int, amount of internal protein; molecular weight is indicated in kDa. Note: Surface levels are calculated by subtracting amount of internal protein from amount of total protein; for details, see *Materials and Methods*. (D) Representative Western blots (WB) for $GABA_AR$ $\alpha4$, $\alpha1$, and $\gamma2$ subunits after co-IP with a $\gamma2$-specific antibody (left) and quantification (right) 24 hours after acute EtOH (E24h)/vehicle. MANOVA, Wilks' $\lambda = 0.217$, $P = 0.022$, $n = 4$. (E) Quantification of the increased association of $\alpha4$ and the decreased association of $\alpha1$ with the $\gamma2$ subunit after CIE in DG and CA1. MANOVA, Wilks' $\lambda = 0.0837$, $P = 0.002$, $n = 4$. (F) Representative Western blots for $GABA_AR$ $\gamma2$, δ, and $\alpha4$ subunits after co-IP with a $\alpha4$-specific antibody (left) and quantification (right) after CIV/CIE. MANOVA, Wilks' $\lambda = 0.392$, $P = 0.038$, $n = 5$. (G) Quantification of the increased association of $\gamma2$ and the decreased association of δ with the $\alpha4$ subunit 24 hours after one dose of EtOH treatment. Wilks' $\lambda = 0.130$, $P = 0.0062$, $n = 4$. Vehicle-treated controls are set as 1.0. Data are mean ± S.E.M. *Significant difference ($P < 0.05$, calculated within MANOVA model) between the treatment and the control.

To verify suggestions from earlier studies that EtOH induced a net switch from $GABA_AR$s composed of $\alpha4\beta\delta$ and $\alpha1\beta\gamma2$ to $\alpha4\beta\gamma2$-containing receptors, coimmunoprecipitation (co-IP) experiments were carried out on solubilized hippocampal membrane proteins from rats. Co-IP experiments using a $\gamma2$-specific antibody after one-dose EtOH showed $\alpha4$ partnering with $\gamma2$ was increased to 217.0% ± 32.4% ($n = 4$), and $\alpha1$ partnering with $\gamma2$ was decreased to 50.6% ± 11.1% ($n = 4$) (Fig. 1D). After CIE, $\alpha4$ showed an increase in $\gamma2$ co-IP to 173.7% ± 16.3% ($n = 4$), whereas $\alpha1$ and $\gamma2$ co-IP was decreased to 52.6% ± 7.0% ($n = 5$) (Fig. 1E). Next, we performed co-IPs with an antibody against the $GABA_AR$ $\alpha4$ subunit after CIE, revealing an increase in $\gamma2$ partnering to 164.6% ± 21.5% ($n = 5$); at the same time, association with the δ subunit was reduced to 54.1% ± 8.7% ($n = 5$) compared with CIV-treated controls (Fig. 1F). Likewise, 24 hours after one-dose EtOH treatment, the $\alpha4$ co-IP with the $\gamma2$ subunit was elevated to 180.9% ± 32.0% ($n = 4$) of vehicle-treated controls; partnering with δ was decreased to 57.9% ± 6.6% ($n = 4$) (Fig. 1G).

Acute and Chronic EtOH Intoxication Increases Surface Levels of $GABA_AR$ $\alpha2$ and $\gamma1$ Subunit Protein. After reports of $GABA_AR$ subunit changes in the the postmortem brain of human alcoholics and animals treated with EtOH (Devaud et al., 1997; Cagetti et al., 2003; Follesa et al., 2004; Jin et al., 2012), we asked whether we could also find changes in total and cell-surface expression of important $GABA_AR$ subunits (Tretter et al., 2008) $\alpha2$ and $\gamma1$ in the rat hippocampus after CIE or a single dose of EtOH. Cross-linking experiments on slices from the DG 24 hours after a single dose of EtOH (5 g/kg) revealed increases in cell surface expression of $\alpha2$ and $\gamma1$ compared with controls (Fig. 2A). The amount of the $\alpha2$ subunit on the cell surface was increased to 176.7% ± 22.9% ($n = 5$), and the amount of the $\gamma1$ subunit was increased to 213.4% ± 28.0% ($n = 5$) in the plasma membrane of the DG (Fig. 2A). In the DG, the total protein level of the $\alpha2$ subunit was unaltered 24 hours after EtOH (94.0 ± 14.1%, $n = 5$). The total amount of $\gamma1$ protein was increased to 199.0 ± 37.4% ($n = 5$) in the DG (Fig. 2B). We next looked at the CA1 and found an increase in cell surface $\alpha2$ to 240.4% ± 50.7% ($n = 6$) and an increase in cell surface $\gamma1$ to 242.9% ± 49.9% ($n = 6$) (Fig. 2C). Total protein levels of $\alpha2$ were not altered (119.8% ± 8.8%, $n = 5$), and total $\gamma1$ in CA1 was increased to 140.0 ± 11.3 ($n = 5$) (Fig. 2B). For CIE experiments, we did not separate the brain regions and used slices from the DG combined with the adjacent CA1. CIE treatment increased cell-surface $\alpha2$ to 228.8% ± 40.4% ($n = 5$) and $\gamma1$ to 173.8% ± 19.2% ($n = 5$) (Fig. 2E). Total $\alpha2$ was not changed after CIE (89.5% ± 17.6%, $n = 4$, $P = 0.665$), whereas total $\gamma1$ was increased to 228.4% ± 48.0% ($n = 4$) (Fig. 2F).

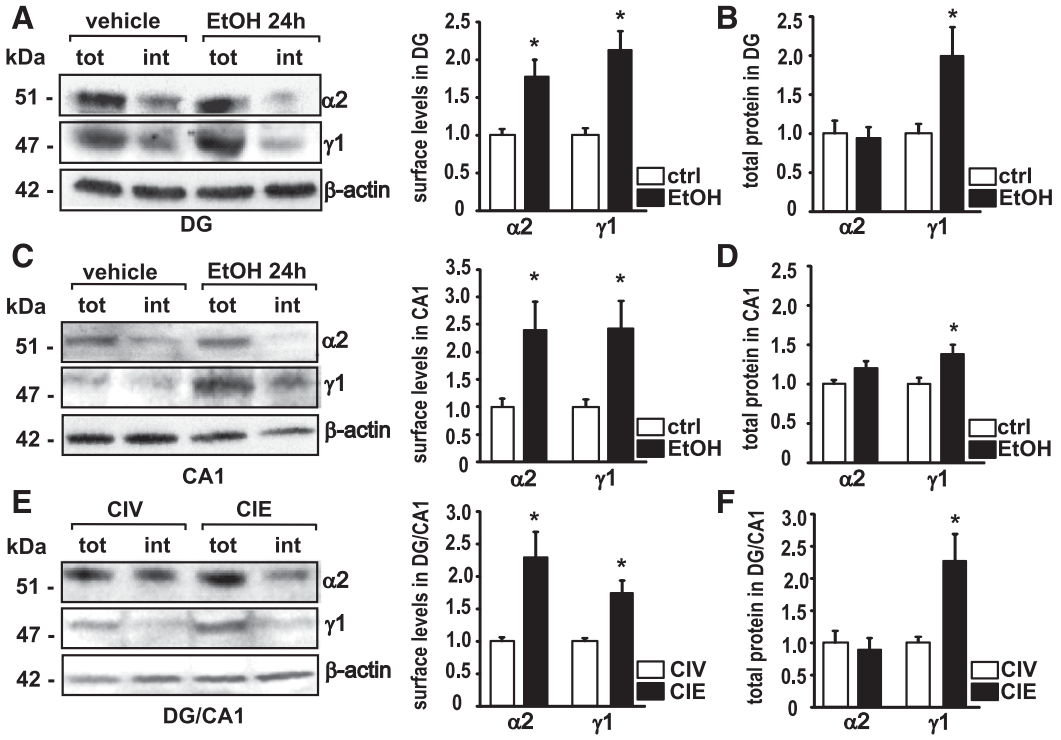

Fig. 2. Administration of acute and chronic EtOH induces an increase in GABA$_A$R α2 and γ1 subunit surface levels. (A) Representative Western blots for α2, γ1, and β-actin after cell-surface cross-linking (left) and quantification (right) 24 hours after a single intoxicating dose of EtOH in the DG. MANOVA, Wilks' $\lambda = 0.226$, $P = 0.0055$, $n = 5$. tot, amount of total protein; int, amount of internal protein. (B) Quantification of the total amount of α2 and γ1 protein measured in DG 24 hours after EtOH intoxication. Wilks' $\lambda = 0.554$, $P = 0.126$, $n = 5$. ctrl, control. (C) Representative Western blots for α2, γ1, and β-actin after cell-surface cross-linking (left) and quantification (right) 24 hours after a single intoxicating dose of EtOH in the CA1. Wilks' $\lambda = 0.443$, $P = 0.0255$, $n = 6$. (D) Quantification of the total amount of α2 and γ1 protein measured in CA1 24 hours after EtOH intoxication. Wilks' $\lambda = 0.478$, $P = 0.0754$, $n = 5$. (E) Representative Western blots for α2, γ1, and β-actin after cell-surface cross-linking (left) and quantification (right) after CIE in the DG + CA1. Wilks' $\lambda = 0.246$, $P = 0.0073$, $n = 5$. (F) Quantification of the total amount of α2 and γ1 protein measured after CIE in DG + CA; tot, total amount of protein; int, intracellular protein content. Wilks' $\lambda = 0.457$, $P = 0.141$, $n = 4$. Controls are set as 1.0%. Data are mean ± S.E.M. *Significant difference ($P < 0.05$, calculated within the MANOVA model) between the treatment versus the control.

CIE and One-Dose EtOH Administration Upregulate GABA$_A$Rs Composed of α2β1γ1 Subunits that Bind to Gephyrin. Co-IP experiments were performed to determine which subunits partner with γ1. Therefore, γ1 co-IPs were carried out in parallel with γ2 co-IPs as a positive control. Western blots were probed for α1, α2, α4, and α5. In contrast to γ2, which was found to associate with different α subunits, γ1 primarily coassembled with the α2 subunit (Fig. 3A). The figure also shows that the γ1 antibody did not co-IP γ2 and vice versa. We next attempted to identify the preferred β subunit partner for the α2γ1-containing GABA$_A$Rs. Membrane proteins were coimmunoprecipitated with β1-, β2-, or β3-specific antibodies and probed for γ1 and γ2. We found that γ1 preferred to form a receptor complex with the β1 subunit, although it was also found to a small extent with β3. Moreover, as is illustrated in Fig. 3B, we found that the γ2 equally partnered with β1 and β3 and somewhat less with β2. These data identify GABA$_A$Rs composed of α2, β1, and γ1 subunits in hippocampal CA1 and the DG regions, which are upregulated after CIE and single-dose EtOH intoxication. The selective partnering of γ1 with α2 allows use of γ1 as a marker for the upregulated pool of cell-surface α2 subunits.

The 93-kDa tubulin-binding protein gephyrin is a marker for GABAergic postsynaptic sites and is assumed to predominantly cluster GABA$_A$R γ2 subunit-containing receptors (Essrich et al., 1998); however, direct interaction is mediated by α subunits (i.e., α1, α2, α3) (Tretter et al., 2008; Saiepour et al., 2010). Since γ1 subunits co-IP with the gephyrin-binding α2 subunit (Fig. 3A), we tested the possibility that γ1-containing GABA$_A$Rs might also bind to gephyrin and found that the hydrophobic interaction between gephyrin and α2 is sensitive to detergents (Tretter et al., 2008). Therefore, we performed co-IP experiments after reversibly cross-linking proteins that are in close vicinity in acute slices to retain unstable, weak interactions (see Materials and Methods). Western blotting with a gephyrin antibody gave the expected 93-kDa signal after using γ2 antibody for co-IP, as well as for the γ1 antibody, whereas the IgG control showed no band (Fig. 3C), suggesting at least some postsynaptic localization of γ1-containing receptors at inhibitory synapses.

Time-Dependent Changes of α4- and α2γ1-Containing GABA$_A$R Subtypes Are Tightly Correlated with Upregulation and Downregulation of EtOH-Sensitive mIPSCs and Withdrawal Anxiety after One or Two Doses of EtOH. As presented already herein, two relatively rare GABA$_A$R subtypes, α4βγ2 and α2β1γ1, were found to be upregulated in the hippocampus postsynaptic membrane after CIE and after a single dose of EtOH in rats. At the same time, mIPSCs became sensitive to enhancement by acute EtOH (50 mM) perfused into the recording chamber, exhibiting a prolonged decay time constant τ and/or an increase in area (charge transfer) of mIPSCs. EtOH-sensitive GABA$_A$Rs are subject to rapid internalization after exposure to high EtOH concentrations (Liang et al., 2007; Shen et al., 2011;

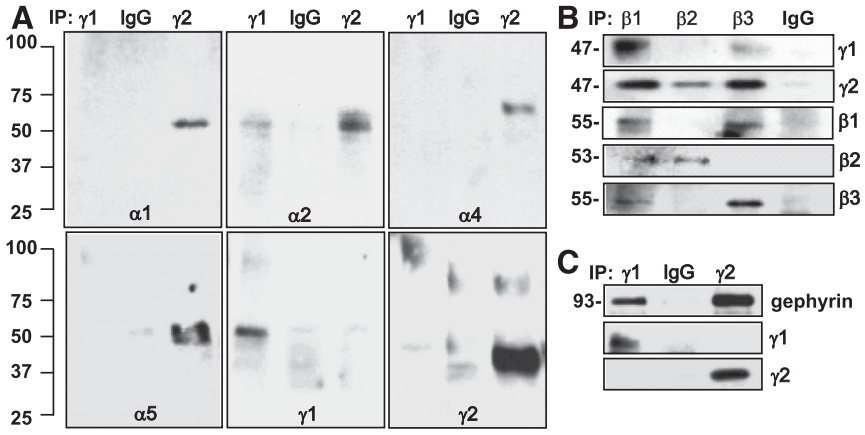

Fig. 3. γ1-Receptors contain α2 and β1 subunits and bind to gephyrin. Solubilized membrane proteins from DG+CA1 slices after CIE were co-immunoprecipitated with antibodies against A. γ1, γ2, or IgG and immunoblotted with antibodies against α1, α2, α4, α5, γ1, and γ2 or B. β1, β2, β3, or IgG and immunoblotted with antibodies against γ1, γ2, β1, β2 and β3 or C. γ1, γ2, and IgG and immunoblotted with antibodies against gephyrin, γ1, and γ2 on the same blot. For C, co-IP experiments were performed after membrane proteins were reversibly cross-linked in acute slices (see Material and Methods). Note, that the β1 antibody gives a signal with β2 and β3; and β3 with β1.

Suryanarayanan et al., 2011; Gonzalez et al., 2012). To identify EtOH-sensitive synaptic $GABA_AR$ dynamic changes after EtOH exposure, we gave rats a "two-pulse" EtOH treatment 48 hours apart (Fig. 4A). At 48 hours (designated 1E48h) after rats received the first EtOH dose (1E), rats received a second EtOH dose (2E) via gavage. GABAergic tonic currents (I_{tonic}) and mIPSCs were patch-clamp-recorded from dentate gyrus granule cells (DGCs) in hippocampal slices obtained from control rats and in rats 48 hours after the first EtOH dose (1E48h), as well as 1 hour (2E1h) and 48 hours (2E48h) after the second dose of EtOH. EtOH sensitivity of $GABA_ARs$ in these four conditions was measured as the responses of I_{tonic} and mIPSCs to acute EtOH (50 mM, E50) perfusion in the recording chamber (Fig. 4A). In controls, the I_{tonic} in response to perfused EtOH was potentiated from 18.9 ± 0.5 to 33.4 ± 1.2 pA (174.9% ± 6.2% of pre-EtOH) but was not changed at 1E48h (E0: 4.0 ± 0.7 pA, E50: 4.3 ± 0.7 pA; 109.9% ± 11.7% of E0), 2E1h (E0: 6.0 ± 0.6 pA, E50: 6.3 ± 0.6 pA; 105.7% ± 3.0% of E0), and at 2E48h (E0: 7.1 ± 1.2 pA, E50: 7.9 ± 1.9 pA; 103.9% ± 9.5% of pre-EtOH) (Fig. 4, B and C). By contrast, in controls, the mIPSC area (charge transfer) was unchanged by EtOH perfusion (103.5% ± 1.3% of E0) but was increased at 1E48h (159.8% ± 12.0% of E0), and at 2E48h (172.5% ± 9.7% of E0). Compared with the 1E48h and 2E48h groups, bath perfused EtOH at 2E1h did not change mIPSC area (109.8% ± 1.7% of pre-EtOH) (Fig. 4, B and C).

To relate the electrophysiology data to $GABA_AR$ subunit composition, we next measured the cell-surface content of α4 (as a marker for $\alpha4\beta\gamma2$ receptors) and γ1 (for $\alpha2\beta1\gamma1$) subtypes at 1E48h, 2E1h, and 2E48h (Fig. 4D). At 2E1h, surface α4-containing $GABA_ARs$ were significantly decreased compared with 1E48h and 2E48h (Fig. 4E). At 2E1h, surface γ1-containing $GABA_ARs$ also robustly decreased compared with 1E48h and 2E48h (Fig. 4E). This finding suggests that both receptor subtypes are affected and become internalized within 1 hour after a second intoxicating EtOH dose; however, this change is transient in that the subtypes reappear 48 hours later. Notably, their cell surface expression is both upregulated and downregulated in concert with the increased EtOH sensitivity of mIPSCs, suggesting that these $GABA_AR$ subtypes might mediate EtOH sensitivity of mIPSCs.

Changes in anxiety-like behaviors have been previously linked to alcohol-induced changes in $GABA_AR$ function (Liang et al., 2006). We measured basal anxiety with the elevated plus maze assay. Control rats (drinking water gavage) spent 49.6% ± 2.3% of total time in open arms versus 50.4% ± 2.3% time in closed arms. The first EtOH dose increased the time spent in open arms to 88.9% ± 3.1% of total time (11.1 ± 3.1% time in closed arms) in the 1E1h group, but 1E48h induced a rebound increase in anxiety as the rat stayed in open arms 8.8% ± 3.8% of total time (91.2% ± 3.8% in closed arms). This rebound increase in anxiety was alleviated by the second EtOH dose. The 2E1h group spent 63.3% ± 5.2% of total time in open arms (36.8% ± 5.3% in closed arms), which was not statistically significant compared with 49.6% ± 2.3% in open arms in control rats; however, 48 hours after the second EtOH dose, basal anxiety was again increased as the rat stayed 23.9% ± 6.2% of total time in open arms (76.6% ± 6.2% in closed arms). Summary statistics of the EPM assays are shown in Fig. 4F. These results suggest that the anxiety levels at different time points after EtOH treatment change concurrently with the postsynaptic $GABA_AR$ dynamic changes.

CIE Induces Upregulation of One or More $GABA_AR$ Subtypes with Slow mIPSC Decay Kinetics. To better understand how changes in subunit combinations alter $GABA_AR$ function and responsiveness to acute EtOH, we measured mIPSCs in DGCs from hippocampal slices of CIV (control) and CIE-treated rats. Recombinant $GABA_ARs$ with differing α subunits, expressed as αβ without γ (Mortensen and Smart, 2006) or with γ2 (Lavoie et al., 1997; McClellan and Twyman, 1999; Vicini, 1999), could be distinguished from each other on the basis of activation and inactivation rates, α1 faster than α2, and can be detected in neurons by the peak shapes of their mIPSCs, which differ between and provide a "fingerprint" for individual α subunits, including α2. Recombinant $\alpha4\beta2\gamma2$ have accelerated deactivation compared with their α1 or α5 counterparts, correlating with upregulated α4 subunit in a hyperexcitable model examining hippocampal slices in a neurosteroid-withdrawn rat (Smith and Gong, 2005). Also, the γ1 subunit-containing receptors (especially with α2) exhibit slower activation and deactivation rates than the respective γ2-containing $GABA_ARs$ expressed in engineered synapses, suggested to be due to a more diffuse clustering (Dixon et al., 2014). mIPSC rise time is sensitive to multiple spatial, physical variables related to synaptic transmission not due to receptor subunit composition (Capogna and Pearce, 2011); however, the decay time is less sensitive to these variables as they are rather random, and yet they are more sensitive to the nature of the postsynaptic receptor channels, such as rates of channel closing and agonist

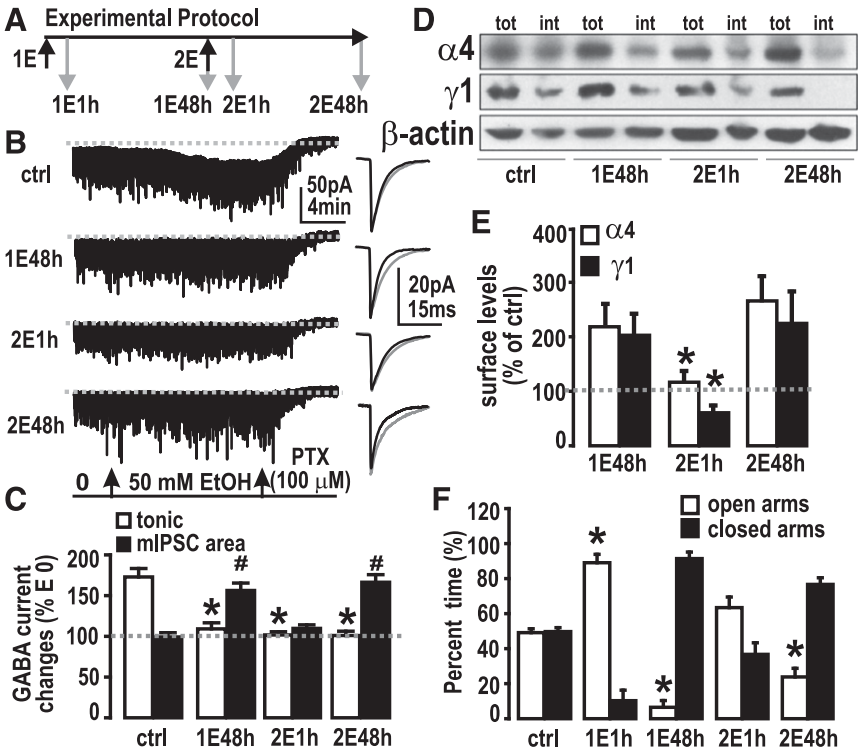

Fig. 4. A second pulse of EtOH reveals further changes in GABA$_A$R physiology, pharmacology, and plasticity, correlated with anxiety-like behavior. (A) "Two-pulse" experimental protocol. Treatment regimen is indicated by black arrows. 1E: First EtOH oral gavage (5 g/kg); 2E: second EtOH gavage. Gray arrows show time points when patch-clamp recordings from DGCs in slices were performed. 1E1h: 1 hour after first EtOH gavage; 1E48h: 48 hours after first EtOH; 2E1h: 1 hour after second EtOH gavage; 2E48h: 48 hours after second EtOH. (B) Effects of acute EtOH (50 mM) applied in the recording chamber on I_{tonic} and mIPSCs. High chloride (135 mM CsCl, refer to *Materials and Methods* section) patch solution was used. The cells were whole-cell voltage-clamped at −70 mV. Gray dashed line is the basal I_{tonic} level after picrotoxin (PTX, 100 μM) application. Representative recordings are shown (left) with the averaged mIPSCs (right) before (black trace) and during (gray trace) EtOH perfusion. ctrl, control (drinking water). (C) Summary of acute EtOH-induced changes in I_{tonic} and mIPSCs. Gray dashed line represents E0 (set as 100%). *$P < 0.05$, significant difference between EtOH treatment versus control in I_{tonic}; #, $P < 0.05$, significant difference between EtOH treatment versus control in mIPSC area (n = 5 or 6/group), one-way ANOVA followed by Dunnett's multiple comparison method comparing three treatment groups with one control group. (D) Representative Western blots for GABA$_A$R α4 and γ1 subunits with their β-actin signals (all from the same blot) after cell-surface cross-linking from control (ctrl), 1E48h, 2E1h, and 2E48h. tot, amount of total protein; int, amount of internal protein. (E) Quantification of surface levels measured by cross-linking experiments. Data are mean ± S.E.M., n = 4–10 rats. *$P < 0.05$ significant decrease versus 1E48h and 2E48h, one-way ANOVA, followed by Holm-Sidak's (pairwise) multiple comparisons test. (F) Anxiety assayed by elevated plus maze (EPM, n = 6/group). Open bars are the time rats spent in open arms (% of total 5-minute monitor time); solid bars are the time spent in closed arms in respective treatment groups. *$P < 0.05$; time spent in open arm of EtOH treatment groups versus control group (drinking water), one-way ANOVA followed by Dunnett's multiple comparison method comparing the four treatment groups with a single control. Note that % time spent in the closed arms is complementary to that in the open arms. Significant % time increase in open arms is equivalent to significant % time decrease in closed arms. Therefore, we omitted statistical tests on time spent in closed arms.

dissociation (Otis and Mody, 1992). Nevertheless, mIPSC shape is highly sensitive to both synaptically released peak GABA concentrations and durations (Lagrange et al., 2007); but according to Kerti-Szigeti and Nusser (2016), "[The] differential expression of GABA$_A$R α subtypes with either a variable or constant ratio from synapse-to-synapse and cell-to-cell, allows them to fulfil individual cellular requirements in network dynamics."

We observed that mIPSCs exhibited a few relatively consistent waveform patterns from the recordings of hippocampal DGCs after CIV and CIE treatments (Fig. 5A). We used the optimally scaled template method (Clements and Bekkers, 1997), implemented in DataView software, to identify kinetic patterns of mIPSCs (e.g., fast rise and fast decay, slow rise and slow decay). Then we used these identified patterns as templates to detect differently shaped mIPSCs in the recording traces. An acceptable error level was set, which is the degree of similarity an event must have to the templates to be included in the search results. The detected mIPSC peak patterns were averaged, mIPSC patterns were classified (Fig. 5B, a-d) and their kinetic decay constants τ determined, and the percentage of abundance was counted (Table 1).

In CIV animals, three distinct mIPSC waveform patterns were detected (Fig. 5B): one standard pattern (a, abundance, ~48%) and the other two displaying a slower decay pattern (c, ~37% and d, ~16%). In CIE animals, we also found three distinct mIPSC shape patterns: a "fast" decay pattern (peak pattern b, ~42%) and two apparently similar to CIV patterns with a slow decay (peak pattern c, ~22%), and a very slow decay pattern (peak pattern d, ~36%) (see Table 1). The standard peak pattern a seen in CIV had disappeared in CIE, whereas the ratio of c to d had reversed, from ~2:1 (CIV) to ~2:3 (CIE). Pattern d had clearly increased in abundance, and pattern c had decreased (see statistics in Table 1).

To better understand the different patterns of peaks possibly carried by particular GABA$_A$R subtypes, we extended this analysis to genetically engineered α4KO mice (Fig. 5). The patterns of mIPSCs in WT mice, untreated pattern a, abundance 46%; pattern c, abundance 36%; pattern d, 18% (Table 1) are similar to CIV rats, whereas α4KO mice showed

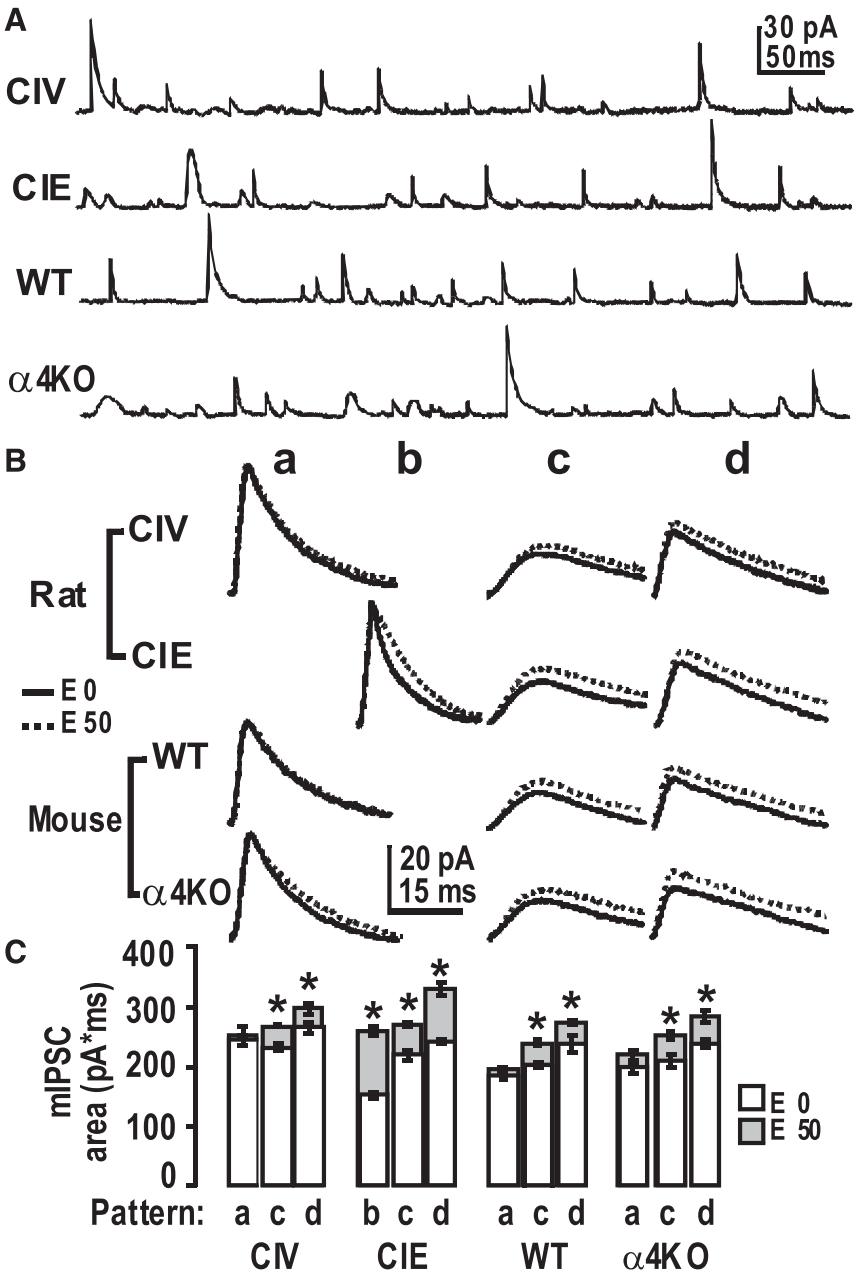

Fig. 5. Pattern analysis reveals different kinetic patterns of mIPSCs after CIE versus CIV and α4KO versus WT. (A) **S**ample recordings of mIPSCs from DGCs. (B) Classifications of patterns of mIPSCs. a, b, c, and d: Averaged mIPSC patterns during recordings before (solid line) and after (dotted line) EtOH application on the hippocampal slice. All averaged mIPSC event patterns were detected by templates from recordings from CIV and CIE rats or α4KO and WT mice using the optimally scaled template algorithm in software DataView (V9.3). The event no. ratios (abundance) of classified mIPSC patterns are shown in Table 1. The scale is for all panels. (C) Responses of mIPSCs charge transfer (area) to acute EtOH application in DGCs. Averaged mIPSC area (mean ± S.E.M.) of different patterns before (empty columns) and after (solid columns) EtOH application. CIV (control); α4KO: α4 subunit knockout mice. E0: without EtOH; E50, in the presence of 50 mM EtOH. $^*P < 0.05$, the area of a pattern in the presence of 50 mM EtOH is statistically different from that of 0 EtOH (two-way repeated measures ANOVA followed by Sidak's method for pairwise multiple comparisons). n = 5 neurons from three rats/group. n = 4 neurons from two mice/group.

mIPSC waveform pattern a (abundance ~36%, Table 1), pattern c (~35%), with increased abundance of pattern d (~29%), and no pattern b (Fig. 5). The absence of pattern b is consistent with the absence of the α4 subtypes.

EtOH (50 mM) perfused into the recording chamber potentiated mIPSCs by prolonging decay time and/or increasing charge transfer (area under the curve), as previously observed (Liang et al., 2006) for CIE rats. We therefore examined whether EtOH (50 mM) application enhanced the current of the various types of mIPSCs detected (Fig. 5B, C). Table 2 shows the decay τ values for the various mIPSCs patterns in the presence and absence of EtOH (50 mM) and the statistical comparisons. We found that acute EtOH potentiated some specific $GABA_AR$ mIPSCs. In CIE rats, waveform pattern b, decay τ1 (in ms) increased from 4.0 ± 0.3 to 8.0 ± 0.3; decay τ2 increased from 12.9 ± 2.2 to 26.9 ± 4.3; and pattern c, decay τ1 increased from 14.6 ± 0.7 to 17.2 ± 0.3; pattern d, only one decay time constant τ increased from 17.4 ± 0.7 to 19.5 ± 0.4. EtOH had no effect on decay times in control CIV rats except pattern c, decay τ1 increased slightly. Similarly, EtOH had no effect on decay times in control WT mice. In α4KO mice, waveform pattern a, decay τ1 increased from 7.1 ± 0.4 to 8.2 ± 0.5; pattern c, decay τ1 increased from 13.8 ± 0.9 to 16.2 ± 1.1; pattern d, τ increased from 16.6 ± 1.1 to 18.4 ± 0.8. The area of the mIPSCs increased greatly in CIE pattern d (Fig. 5), as did its abundance (Table 1). This in vitro sensitivity to EtOH modulation correlated in time with the upregulation and downregulation of the α4- and especially the α2-containing $GABA_AR$ subtype species (Fig. 4). Figure 6 shows a reasonable hypothesis of $GABA_AR$ plasticity induced by EtOH in rat hippocampus (updated from Liang et al., 2007), which shows how synaptic and extrasynaptic $GABA_AR$ subtypes change rapidly in surface expression after in vivo exposure to EtOH and that the plastic changes become persistent after CIE

TABLE 1

Characterization of mIPSC waveforms and decay times in DG granule cells from hippocampal slices

Numbers are mean ± S.E.M. τ1 and τ2 are time constants when the decay of mIPSCs was fitted with two exponentials. Decay of mIPSCs in pattern d was fitted well with only one exponential. Abd (abundance): percentage of mIPSC numbers of a specific pattern (a, b, c, or d) versus total number of mIPSCs (patterns a + b + c + d). analyzed from a neuron.

	Pattern a Abd			Pattern b			Pattern c			Pattern d	
	τ1 (ms)	*τ2 (ms)*	*Abd (%)*	*τ1 (ms)*	*τ2 (ms)*	*Abd (%)*	*τ1 (ms)*	*τ2 (ms)*	*Abd (%)*	*τ (ms)*	*Abd (%)*
CIV	7.8 ± 0.4	32.0 ± 11.1	47.8 ± 2.6				14.1 ± 1.2	54.9 ± 11.3	36.6 ± 1.9	16.9 ± 0.6	15.6 ± 1.9
CIE				4.0 ± 0.3	12.9 ± 2.2	42.6 ± 0.9	14.6 ± 0.7	70.4 ± 9.2	21.8 ± 1.8*	17.4 ± 0.7	35.6 ± 2.4*
WT	7.6 ± 0.5	37.1 ± 10.5	46.2 ± 2.2				13.7 ± 0.6	35.9 ± 8.9	36.3 ± 1.9	17.0 ± 0.5	17.5 ± 0.7
α4KO	7.1 ± 0.4	28.0 ± 8.6	35.5 ± 1.9†				13.8 ± 0.9	35.4 ± 8.6	35.3 ± 2.9	16.6 ± 1.1	29.2 ± 1.1†

†$P < 0.05$, Abd of a pattern in α4KO group statistically different from that of WT group (one-way ANOVA followed by Sidak method for pairwise multiple comparisons). *Abd of every pattern is not statistically significant between CIV and WT group. $n = 6$ neurons from three rats/group, $n = 5$ neurons from two mice/group.

treatment. Note that in this simplified cartoon we have grouped all the game players in a single synapse, which is not likely to be the actual situation.

Discussion

We have shown that two novel GABA$_A$R subtypes are upregulated after acute EtOH treatment and CIE. Cell-surface levels of both subtypes are tightly synchronized over one- or two-dose EtOH administration, with changes in anxiety behavior and the abundance of EtOH-enhanced mIPSCs. We directly related changes in surface expression of GABA$_A$R subunits (downregulation of α1 and δ, upregulation of α4, α2, γ1, and γ2) with a decrease in heteropentameric $\alpha4\beta\delta$- and $\alpha1\beta\gamma2$-containing GABA$_A$Rs and an increase in postsynaptic $\alpha4\beta\gamma2$- and $\alpha2\beta1\gamma1$-containing GABA$_A$Rs in hippocampal neurons (Fig. 6). EtOH-induced decreases in α1 and δ subunits and increased α4 and γ2 are also found in other brain regions, including the basolateral amygdala (Diaz et al., 2011; Lindemeyer et al., 2014) and nucleus accumbens (Liang et al., 2014), whereas α2 was downregulated in the amygdala and α5 was upregulated in the nucleus accumbens. In this study, decreased extrasynaptic $\alpha4\beta\delta$ GABA$_A$Rs correlated with decreased GABA$_A$R-mediated I_{tonic} and loss of its EtOH sensitivity. Upregulated α2 subtypes correlated with the appearance of synaptic currents enhanced by EtOH (>10 mM). EtOH-enhanced mIPSCs have also been observed in untreated α4KO mice (Liang et al., 2008; Suryanarayanan et al., 2011), in which the EtOH-sensitive subtype cannot contain α4. The α2 subunit is colocalized with gephyrin and presynaptic glutamic acid decarboxylase at both DGC cell bodies and axon initial segments (Kerti-Szigeti and Nusser, 2016) and is upregulated in the hippocampus of α4KO mice (Liang et al., 2008; Suryanarayanan et al., 2011).

The decrease in $\alpha1\beta\gamma2$- and gain of $\alpha4\beta\gamma2$- and $\alpha2\beta1\gamma1$-containing GABA$_A$Rs change the kinetics and pharmacologic properties of mIPSCs. We previously found decreased diazepam or zolpidem enhancement of mIPSC decay constants and a markedly increased area by the imidazobenzodiazepine partial inverse agonist Ro15-4513 in hippocampal slices after CIE (Cagetti et al., 2003; Liang et al., 2004, 2007, 2009) and single-dose treatment in vivo (Liang et al., 2007). These pharmacologic and subunit changes were reproduced in primary cultured embryonic hippocampal neurons after 15 days in vitro, 24 hours after exposure for 30 minutes to EtOH (50 mM) (Shen et al., 2011). In recombinant systems, GABA$_A$Rs containing α4/α6 when expressed with the γ2 subunit are insensitive to traditional benzodiazepine drugs and zolpidem, whereas Ro15-4513 acts as an agonist (Knoflach et al., 1996; Wafford et al., 1996). Recombinant GABA$_A$Rs containing the γ1 subunit show slightly different BZ pharmacology from γ2, including agonism by Ro15-4513 (Puia et al., 1991; Wafford et al., 1993). Ro15-4513 at 1 μM slightly potentiates $\alpha2\beta1\gamma1$ receptors expressed in *Xenopus* oocytes (Wafford et al., 1993), which indicates that $\alpha2\beta1\gamma1$ and $\alpha4\beta\gamma2$ receptor subtypes have a similar, not easily distinguishable, pharmacologic profile.

We tried to identify the EtOH-sensitive GABA$_A$R (presumably either $\alpha4\beta\gamma2$or $\alpha2\beta1\gamma1$) by two-pulse EtOH experiments using the assumption, that subtypes responding to EtOH will become internalized within 1 hour, as demonstrated for δ-containing

TABLE 2

Responses of mIPSCs to acute drug (EtOH) application in DGCs

τ1 and τ2 are time constants (mean ± S.E.M.) when the decay of mIPSCs was fitted with two exponentials. Decay of mIPSCs in pattern d was fitted well with only one exponential (MiniAnalysis program V6.07). α4KO, α4 subunit knockout mice; E0, without EtOH; E50, in the presence of 50 mM EtOH.

	Pattern a		Pattern b		Pattern c		Pattern d
	τ1 (ms)	*τ2 (ms)*	*τ1 (ms)*	τ2 (ms)	*τ1 (ms)*	*τ2 (ms)*	*τ (ms)*
CIV E0	7.8 ± 0.4	32.0 ± 11.1			14.1 ± 1.2	54.9 ± 11.3	16.9 ± 0.6
E50	8.0 ± 0.4	60.3 ± 11.6			16.3 ± 0.7*	58.4 ± 14.6	18.2 ± 0.5
CIE E0			4.0 ± 0.3	12.9 ± 2.2	14.6 ± 0.7	70.4 ± 9.2	17.4 ± 0.7
E50			8.0 ± 0.3*	26.9 ± 4.3*	17.2 ± 0.3*	73.1 ± 12.5	19.5 ± 0.4*
WT E0	7.6 ± 0.5	37.1 ± 10.5			13.7 ± 0.6	35.9 ± 8.9	17.0 ± 0.5
E50	7.7 ± 0.4	53.9 ± 3.6			14.8 ± 0.5	50.7 ± 13.5	18.0 ± 0.5
α4KO E0	7.1 ± 0.4	28.0 ± 8.6			13.8 ± 0.9	35.4 ± 8.6	16.6 ± 1.1
E50	8.2 ± 0.5*	48.0 ± 12.4			16.2 ± 1.1*	63.7 ± 19.9	18.4 ± 0.8*

*$P < 0.05$, the decay time constant of a pattern in the presence of 50 mM EtOH is statistically different from that of 0 EtOH (two-way repeated measures ANOVA, followed by Sidak method for pairwise multiple comparison). $n = 6$ neurons from three rats/group. $n = 5$ neurons from two mice/group.

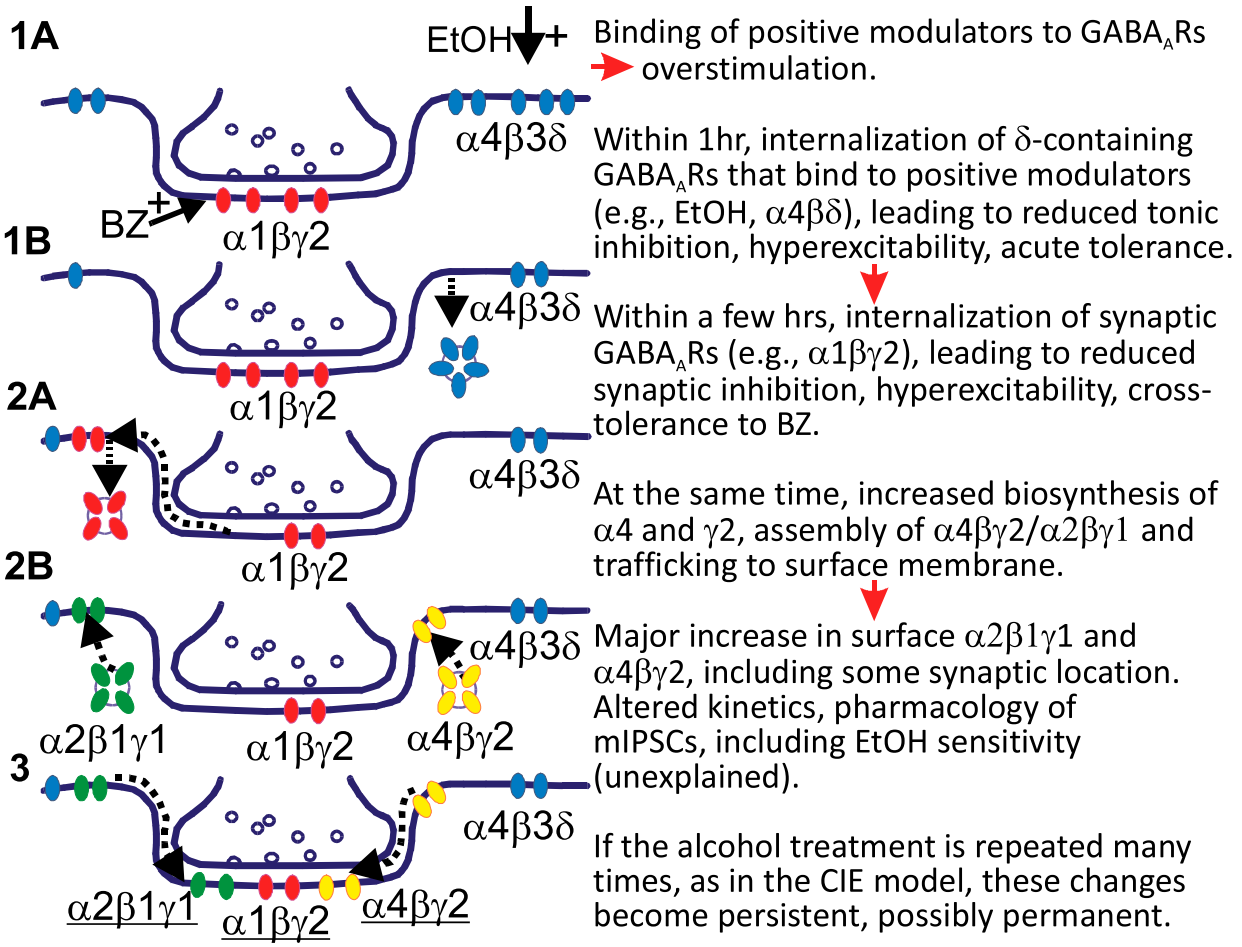

Fig. 6. Hypothetical model of GABA$_A$R subunit plasticity seen within two days following a single intoxicating dose of EtOH to rats leading to changes of physiopharmacologic properties in GABAergic ionotropic receptor-mediated inhibitory synaptic transmission in hippocampus.

GABA$_A$Rs after one-pulse EtOH (Shen et al., 2011); the reversible loss of EtOH sensitivity of mIPSCs at 1 hour after the second EtOH dose paralleled reversible decreases in both α4- and α2γ1-containing surface-expressed GABA$_A$Rs. In addition, the increased anxiety 48 hours after the first dose of EtOH could be partially alleviated by the second EtOH dose, measured after 1 hour. Therefore, the two-pulse EtOH experiments failed to distinguish which receptor subtypes mediate EtOH sensitivity; however, mIPSC pattern recognition analysis suggested that both α2 and α4 subtypes are involved.

CIE-Induced mIPSCs with Slow Decay Kinetics, Enhanced by EtOH in the Recording Chamber, Correlate with Upregulated α2 Subunits. We previously reported (Liang et al., 2006) a difference between the decay rates of mIPSCs in DGCs in CIE compared with CIV controls. The control mIPSCs, which are sensitive to BZ drugs and insensitive to EtOH, were downregulated by CIE treatment in parallel with the α1 subunit. The CIE-induced averaged mIPSCs were sharper, faster decaying, insensitive to BZ, but enhanced by Ro15-4513 and enhanced EtOH, and correlated with upregulated α4 subunit.

In the present study, we analyzed patch-clamp recordings from hippocampal DGCs in CIE-treated rats and controls using an optimally scaled template algorithm (Clements and Bekkers, 1997) implemented in DataView software. We mentioned above that although mIPSC kinetics are sensitive to multiple anatomic variables affecting transmitter concentrations and duration during synaptic transmission, the decay time is very sensitive to the nature of the postsynaptic receptor channels and can give clues to the nature of GABA$_A$R α subtypes (Otis and Mody, 1992; McClellan and Twyman, 1999; Vicini, 1999; Lagrange et al., 2007; Kerti-Szigeti and Nusser, 2016).

We were able to detect mIPSCs of distinct waveforms consistent with the heterogeneity of GABA$_A$Rs formed from different α subunits. These were found consistently over multiple recordings in different DGCs and thus are unlikely to result from anatomic variables. We confirmed that control, CIV, and WT animals were enriched in typically shaped mIPSCs (peak a in Fig. 5 and Table 1), which showed no enhancement by EtOH in the recording chamber and downregulated by CIE, consistent with the α1$\beta\gamma$2 GABA$_A$R subtype. CIE treatment induced a new rapidly decaying peak, now described as pattern b in Fig. 5, which correlated with the appearance of upregulated α4$\beta\gamma$2 GABA$_A$R subtype, showing some enhancement by EtOH. Consistent with this, pattern b is missing in the α4KO mouse (Fig. 5).

The averaged shapes must contain some contribution from α2. Numerous mIPSC waveform events with slow decay consistent with the presence of α2 GABA$_A$Rs were detectable in CIV controls, and these were increased in CIE rats. Since α2 is upregulated in CIE rats, as are EtOH enhanced, slow-decay mIPSCs, and likewise in untreated α4KO mice as shown by Western blot analysis (Suryanarayanan et al., 2011) and by

immunohistochemistry (Houser CR, Liang J, and Olsen RW, unpublished), we posit that α2 contributes to these mIPSCs. Peak pattern c- and d-like slow-decay mIPSCs were found in CIV and CIE rats, as well as WT and α4KO mice; both were enhanced by mM EtOH in the recording chamber. Comparing the abundance of kinetic patterns in the four conditions (Table 1), we conclude that the sum of pattern c and d correlate with upregulated α2 subunit-containing GABA$_A$Rs. Further, the abundance ratio of peaks d to c is elevated in both CIE rats and α4KO mice (Fig. 5; Table 1), and this upregulation of peak 'd' correlates with the averaged mIPSCs exhibiting greater EtOH enhancement (Fig. 6). It is likely that the EtOH-sensitive mIPSCs with unusually slow decay (peak pattern d) are due to α2, perhaps demonstrating an unusual subunit combination (e.g., α2β1γ1), or some other 'abnormal' postsynaptic membrane structure. Interestingly, in DGCs of both untreated δ- and α4KO mice, mIPSC charge transfer is increased by acute EtOH in the recording chamber, which is not observed in WT animals (Liang et al., 2006; Liang et al., 2008; Suryanarayanan et al., 2011). We find an increased amount of the GABA$_A$R γ1 subunit in δKO and α4KO mice compared with WT by Western blot analysis (Lindemeyer AK, Liang J, and Olsen RW, unpublished). It is tempting to speculate that α2βγ1 receptors may mediate EtOH sensitivity in these animals. Future work on genetically engineered rodents should allow proof of which GABA$_A$R subtypes are critical for the relevant plasticity.

Relationship between Alcohol Use Disorder and the Gene Cluster Encoding GABA$_A$R Subunits α2, β1, γ1, and α4 on Human Chromosome 4. There is growing evidence that alcoholism as a complicated behavioral disorder has complex genetic involvement. In particular, genes encoding the chromosome 4 cluster of GABA$_A$R subunits *GABRA4, GABRA2, GABRB1, and GABRG1* are genetically linked to certain aspects of alcoholism in humans. Because coregulation of GABA$_A$R subunits within gene clusters has been reported during development (Fillman et al., 2010), there may be some combination of these gene products acting together functionally in some way to affect alcohol behavior. Single nucleotide polymorphisms in the chromosome 4 GABA$_A$R subunit genes are highly associated with alcohol abuse and dependence (Porjesz et al., 2002; Edenberg et al., 2004; Enoch et al., 2009; Borghese and Harris, 2012). Postmortem brain of human alcoholics exhibits elevated α1, α4, α5, and especially β1 and γ1 mRNA in the hippocampus (Jin et al., 2012).

The α2 subunit has been shown by mouse genetic engineering to be required for the anxiolytic efficacy and dependence liability of benzodiazepines (Rudolph and Knoflach, 2011; Engin et al., 2016). Gephyrin-binding subunits (α2) of GABA$_A$Rs are important for receptor dynamics critical for plasticity phenomena such as inhibitory LTP (Petrini et al., 2014; Tyagarajan and Fritschy, 2014). The α2 candidate partner (but rare) γ1 subunit is abundant and functional in the central amygdala (Esmaeili et al., 2009); knockdown of α2 expression in this area resulted in reduction of binge drinking (Liu et al., 2011). The hippocampus likewise participates in neurocircuitry of drug craving and relapse (Koob and Volkow, 2010). Our studies reveal GABA$_A$Rs as novel targets of neuronal adaptations in response to EtOH, probably important for understanding alcohol-induced memory loss and drug-seeking behavior during abstinence and facilitating the development of therapeutic alcohol use disorder treatment.

Acknowledgments

The authors thank Werner Sieghart for supplying the GABA$_A$ receptor subunit-specific antibodies.

Authoship Contributions

Participated in research design: Lindemeyer, Shen, Shao, Spigelman, Olsen, Liang.

Conducted experiments: Lindemeyer (biochemistry), Shen (electrophysiology), Yazdani (behavior), Spigelman (electrophysiology), Liang (electrophysiology and behavior).

Performed data analysis: Lindemeyer, Shen, Shao, Spigelman, Olsen, Liang.

Wrote or contributed to the writing of the manuscript: Lindemeyer, Shao, Spigelman, Davies, Olsen, Liang.

References

Borghese CM and Harris RA (2012) Alcohol dependence and genes encoding α2 and γ1 GABA$_A$ receptor subunits: insights from humans and mice. *Alcohol Res* **34**: 345–353.

Borghese CM, Storustovu S, Ebert B, Herd MB, Belelli D, Lambert JJ, Marshall G, Wafford KA, and Harris RA (2006) The delta subunit of gamma-aminobutyric acid type A receptors does not confer sensitivity to low concentrations of ethanol. *J Pharmacol Exp Ther* **316**:1360–1368.

Cagetti E, Liang J, Spigelman I, and Olsen RW (2003) Withdrawal from chronic intermittent ethanol treatment changes subunit composition, reduces synaptic function, and decreases behavioral responses to positive allosteric modulators of GABA$_A$ receptors. *Mol Pharmacol* **63**:53–64.

Capogna M and Pearce RA (2011) GABA $_{A,slow}$: causes and consequences. *Trends Neurosci* **34**:101–112.

Chandra D, Jia F, Liang J, Peng Z, Suryanarayanan A, Werner DF, Spigelman I, Houser CR, Olsen RW, Harrison NL, et al. (2006) GABA$_A$ receptor alpha 4 subunits mediate extrasynaptic inhibition in thalamus and dentate gyrus and the action of gaboxadol. *Proc Natl Acad Sci USA* **103**:15230–15235.

Clements JD and Bekkers JM (1997) Detection of spontaneous synaptic events with an optimally scaled template. *Biophys J* **73**:220–229.

Devaud LL, Fritschy JM, Sieghart W, and Morrow AL (1997) Bidirectional alterations of GABA$_A$ receptor subunit peptide levels in rat cortex during chronic ethanol consumption and withdrawal. *J Neurochem* **69**:126–130.

Diaz MR, Christian DT, Anderson NJ, and McCool BA (2011) Chronic ethanol and withdrawal differentially modulate lateral/basolateral amygdala paracapsular and local GABAergic synapses. *J Pharmacol Exp Ther* **337**:162–170.

Dixon C, Sah P, Lynch JW, and Keramidas A (2014) GABA$_A$ receptor α and γ subunits shape synaptic currents via different mechanisms. *J Biol Chem* **289**: 5399–5411.

Ebert V, Scholze P, and Sieghart W (1996) Extensive heterogeneity of recombinant gamma-aminobutyric acid A receptors expressed in alpha 4 beta 3 gamma 2-transfected human embryonic kidney 293 cells. *Neuropharmacology* **35**:1323–1330.

Edenberg HJ, Dick DM, Xuei X, Tian H, Almasy L, Bauer LO, Crowe RR, Goate A, Hesselbrock V, Jones K, et al. (2004) Variations in GABRA2, encoding the alpha 2 subunit of the GABA$_A$ receptor, are associated with alcohol dependence and with brain oscillations. *Am J Hum Genet* **74**:705–714.

Engin E, Smith KS, Gao Y, Nagy D, Foster RA, Tsvetkov E, Keist R, Crestani F, Fritschy JM, Bolshakov VY, et al. (2016) Modulation of anxiety and fear via distinct intrahippocampal circuits. *eLife* **5**:e14120.

Enoch MA, Hodgkinson CA, Yuan Q, Albaugh B, Virkkunen M, and Goldman D (2009) GABRG1 and GABRA2 as independent predictors for alcoholism in two populations. *Neuropsychopharmacology* **34**:1245–1254.

Esmaeili A, Lynch JW, and Sah P (2009) GABA$_A$ receptors containing gamma1 subunits contribute to inhibitory transmission in the central amygdala. *J Neurophysiol* **101**:341–349.

Essrich C, Lorez M, Benson JA, Fritschy JM, and Lüscher B (1998) Postsynaptic clustering of major GABA$_A$ receptor subtypes requires the gamma 2 subunit and gephyrin. *Nat Neurosci* **1**:563–571.

Fillman SG, Duncan CE, Webster MJ, Elashoff M, and Weickert CS (2010) Developmental co-regulation of the beta and gamma GABA$_A$ receptor subunits with distinct alpha subunits in the human dorsolateral prefrontal cortex. *Int J Dev Neurosci* **28**:513–519.

Follesa P, Biggio F, Mancuso L, Cabras S, Caria S, Gorini G, Manca A, Orru A, and Biggio G (2004) Ethanol withdrawal-induced up-regulation of the alpha2 subunit of the GABA$_A$ receptor and its prevention by diazepam or gamma-hydroxybutyric acid. *Brain Res Mol Brain Res* **120**:130–137.

Gonzalez C, Moss SJ, and Olsen RW (2012) Ethanol promotes clathrin adaptor-mediated endocytosis via the intracellular domain of delta-containing GABA$_A$ receptors. *J Neurosci* **32**:17874–17881.

Grosshans DR, Clayton DA, Coultrap SJ, and Browning MD (2002) Analysis of glutamate receptor surface expression in acute hippocampal slices. *Sci STKE* **2002**:pl8.

Hanchar HJ, Dodson PD, Olsen RW, Otis TS, and Wallner M (2005) Alcohol-induced motor impairment caused by increased extrasynaptic GABA$_A$ receptor activity. *Nat Neurosci* **8**:339–345.

Jechlinger M, Pelz R, Tretter V, Klausberger T, and Sieghart W (1998) Subunit composition and quantitative importance of hetero-oligomeric receptors: GABA$_A$ receptors containing alpha6 subunits. *J Neurosci* **18**:2449–2457.

Jin Z, Bazov I, Kononenko O, Korpi ER, Bakalkin G, and Birnir B (2012) Selective changes of GABA$_A$ channel subunit mRNAs in the hippocampus and orbitofrontal cortex but not in prefrontal cortex of human alcoholics. *Front Cell Neurosci* **5**:30.

Jones A, Korpi ER, McKernan RM, Pelz R, Nusser Z, Mäkelä R, Mellor JR, Pollard S, Bahn S, Stephenson FA, et al. (1997) Ligand-gated ion channel subunit partnerships: $GABA_A$ receptor α6 subunit gene inactivation inhibits δ subunit expression. *J Neurosci* **17**:1350–1362.

Kerti-Szigeti K and Nusser Z (2016) Similar $GABA_A$ receptor subunit composition in somatic and axon initial segment synapses of hippocampal pyramidal cells. *eLife* **5**: e18426.

Khom S, Baburin I, Timin EN, Hohaus A, Sieghart W, and Hering S (2006) Pharmacological properties of $GABA_A$ receptors containing γ1 subunits. *Mol Pharmacol* **69**:640–649.

Knoflach F, Benke D, Wang Y, Scheurer L, Luddens H, Hamilton BJ, Carter DB, Mohler H, and Benson JA (1996) Pharmacological modulation of the diazepam-insensitive recombinant gamma-aminobutyric acid A receptors alpha 4 beta 2 gamma 2 and alpha 6 beta 2 gamma 2. *Mol Pharmacol* **50**:1253–1261.

Koob GF and Volkow ND (2010) Neurocircuitry of addiction. *Neuropsychopharmacology* **35**:217–238.

Kumar S, Porcu P, Werner DF, Matthews DB, Diaz-Granados JL, Helfand RS, and Morrow AL (2009) The role of $GABA_A$ receptors in the acute and chronic effects of ethanol: a decade of progress. *Psychopharmacology (Berl)* **205**:529–564.

Lagrange AH, Botzolakis EJ, and Macdonald RL (2007) Enhanced macroscopic desensitization shapes the response of alpha4 subtype-containing $GABA_A$ receptors to synaptic and extrasynaptic GABA. *J Physiol* **578**:655–676.

Lavoie AM, Tingey JJ, Harrison NL, Pritchett DB, and Twyman RE (1997) Activation and deactivation rates of recombinant $GABA_A$ receptor channels are dependent on alpha-subunit isoform. *Biophys J* **73**:2518–2526.

Liang J, Cagetti E, Olsen RW, and Spigelman I (2004) Altered pharmacology of synaptic and extrasynaptic $GABA_A$ receptors on CA1 hippocampal neurons is consistent with subunit changes in a model of alcohol withdrawal and dependence. *J Pharmacol Exp Ther* **310**:1234–1245.

Liang J, Lindemeyer AK, Suryanarayanan A, Meyer EM, Marty VN, Ahmad SO, Shao XM, Olsen RW, and Spigelman I (2014) Plasticity of $GABA_A$ receptor-mediated neurotransmission in the nucleus accumbens of alcohol-dependent rats. *J Neurophysiol* **112**:39–50.

Liang J, Spigelman I, and Olsen RW (2009) Tolerance to sedative/hypnotic actions of GABAergic drugs correlates with tolerance to potentiation of extrasynaptic tonic currents of alcohol-dependent rats. *J Neurophysiol* **102**:224–233.

Liang J, Suryanarayanan A, Abriam A, Snyder B, Olsen RW, and Spigelman I (2007) Mechanisms of reversible $GABA_A$ receptor plasticity after ethanol intoxication. *J Neurosci* **27**:12367–12377.

Liang J, Suryanarayanan A, Chandra D, Homanics GE, Olsen RW, and Spigelman I (2008) Functional consequences of $GABA_A$ receptor alpha 4 subunit deletion on synaptic and extrasynaptic currents in mouse dentate granule cells. *Alcohol Clin Exp Res* **32**:19–26.

Liang J, Zhang N, Cagetti E, Houser CR, Olsen RW, and Spigelman I (2006) Chronic intermittent ethanol-induced switch of ethanol actions from extrasynaptic to synaptic hippocampal $GABA_A$ receptors. *J Neurosci* **26**:1749–1758.

Lindemeyer AK, Liang J, Marty VN, Meyer EM, Suryanarayanan A, Olsen RW, and Spigelman I (2014) Ethanol-induced plasticity of $GABA_A$ receptors in the basolateral amygdala. *Neurochem Res* **39**:1162–1170.

Liu J, Yang AR, Kelly T, Puche A, Esoga C, June, JrHL, Elnabawi A, Merchenthaler I, Sieghart W, June, SrHL, et al. (2011) Binge alcohol drinking is associated with $GABA_A$ α2-regulated Toll-like receptor 4 (TLR4) expression in the central amygdala. *Proc Natl Acad Sci USA* **108**:4465–4470.

Lovinger DM and Homanics GE (2007) Tonic for what ails us? high-affinity $GABA_A$ receptors and alcohol. *Alcohol* **41**:139–143.

McClellan AM and Twyman RE (1999) Receptor system response kinetics reveal functional subtypes of native murine and recombinant human $GABA_A$ receptors. *J Physiol* **515**:711–727.

McLean PJ, Farb DH, and Russek SJ (1995) Mapping of the alpha 4 subunit gene (GABRA4) to human chromosome 4 defines an alpha 2-alpha 4-beta 1-gamma 1 gene cluster: further evidence that modern $GABA_A$ receptor gene clusters are derived from an ancestral cluster. *Genomics* **26**:580–586.

Mody I, Glykys J, and Wei W (2007) A new meaning for "gin & tonic": tonic inhibition as the target for ethanol action in the brain. *Alcohol* **41**:145–153.

Mortensen M and Smart TG (2006) Extrasynaptic alphabeta subunit GABAA receptors on rat hippocampal pyramidal neurons. *J Physiol* **577**:841–856.

Nusser Z, Sieghart W, and Somogyi P (1998) Segregation of different $GABA_A$ receptors to synaptic and extrasynaptic membranes of cerebellar granule cells. *J Neurosci* **18**:1693–1703.

O'Dell LE, Roberts AJ, Smith RT, and Koob GF (2004) Enhanced alcohol self-administration after intermittent versus continuous alcohol vapor exposure. *Alcohol Clin Exp Res* **28**:1676–1682.

Olsen RW and Sieghart W (2008) International Union of Pharmacology. LXX. Subtypes of gamma-aminobutyric acid(A) receptors: classification on the basis of subunit composition, pharmacology, and function. Update. *Pharmacol Rev* **60**:243–260.

Olsen RW and Spigelman I (2012) $GABA_A$ receptor plasticity in Alcohol Withdrawal, in *Jasper's Basic Mechanisms of the Epilepsies* (Noebels JL, Avoli M, Rogawski MA, Olsen RW, and Delgado-Escueta AV, eds),National Institutes of Health, Bethesda, MD.

Otis TS and Mody I (1992) Modulation of decay kinetics and frequency of $GABA_A$ receptor-mediated spontaneous inhibitory postsynaptic currents in hippocampal neurons. *Neuroscience* **49**:13–32.

Petrini EM, Ravasenga T, Hausrat TJ, Iurilli G, Olcese U, Racine V, Sibarita JB, Jacob TC, Moss SJ, Benfenati F, et al. (2014) Synaptic recruitment of gephyrin regulates surface $GABA_A$ receptor dynamics for the expression of inhibitory LTP. *Nat Commun* **5**:3921.

Pöltl A, Hauer B, Fuchs K, Tretter V, and Sieghart W (2003) Subunit composition and quantitative importance of $GABA_A$ receptor subtypes in the cerebellum of mouse and rat. *J Neurochem* **87**:1444–1455.

Porjesz B, Begleiter H, Wang K, Almasy L, Chorlian DB, Stimus AT, Kuperman S, O'Connor SJ, Rohrbaugh J, Bauer LO, et al. (2002) Linkage and linkage disequilibrium mapping of ERP and EEG phenotypes. *Biol Psychol* **61**:229–248.

Puia G, Vicini S, Seeburg PH, and Costa E (1991) Influence of recombinant gamma-aminobutyric acid-A receptor subunit composition on the action of allosteric modulators of GABA-gated Cl- currents. *Mol Pharmacol* **39**:691–696.

Rimondini R, Sommer W, and Heilig M (2003) A temporal threshold for induction of persistent alcohol preference: behavioral evidence in a rat model of intermittent intoxication. *J Stud Alcohol* **64**:445–449.

Rudolph U and Knoflach F (2011) Beyond classical benzodiazepines: novel therapeutic potential of $GABA_A$ receptor subtypes. *Nat Rev Drug Discov* **10**:685–697.

Saiepour L, Fuchs C, Patrizi A, Sassoè-Pognetto M, Harvey RJ, and Harvey K (2010) Complex role of collybistin and gephyrin in $GABA_A$ receptor clustering. *J Biol Chem* **285**:29623–29631.

Schwarzer C, Tsunashima K, Wanzenböck C, Fuchs K, Sieghart W, and Sperk G (1997) $GABA_A$ receptor subunits in the rat hippocampus II: altered distribution in kainic acid-induced temporal lobe epilepsy. *Neuroscience* **80**:1001–1017.

Shen Y, Lindemeyer AK, Spigelman I, Sieghart W, Olsen RW, and Liang J (2011) Plasticity of $GABA_A$ receptors after ethanol pre-exposure in cultured hippocampal neurons. *Mol Pharmacol* **79**:432–442.

Simms JA, Steensland P, Medina B, Abernathy KE, Chandler LJ, Wise R, and Bartlett SE (2008) Intermittent access to 20% ethanol induces high ethanol consumption in Long-Evans and Wistar rats. *Alcohol Clin Exp Res* **32**:1816–1823.

Simon J, Wakimoto H, Fujita N, Lalande M, and Barnard EA (2004) Analysis of the set of $GABA_A$ receptor genes in the human genome. *J Biol Chem* **279**: 41422–41435.

Slany A, Zezula J, Tretter V, and Sieghart W (1995) Rat β 3 subunits expressed in human embryonic kidney 293 cells form high affinity [^{35}S]t-butylbicyclophosphorothionate binding sites modulated by several allosteric ligands of γ-aminobutyric acid type A receptors. *Mol Pharmacol* **48**:385–391.

Smith SS and Gong QH (2005) Neurosteroid administration and withdrawal alter $GABA_A$ receptor kinetics in CA1 hippocampus of female rats. *J Physiol* **564**: 421–436.

Sundstrom-Poromaa I, Smith DH, Gong QH, Sabado TN, Li X, Light A, Wiedmann M, Williams K, and Smith SS (2002) Hormonally regulated α(4)β(2)δ $GABA_A$ receptors are a target for alcohol. *Nat Neurosci* **5**:721–722.

Suryanarayanan A, Liang J, Meyer EM, Lindemeyer AK, Chandra D, Homanics GE, Sieghart W, Olsen RW, and Spigelman I (2011) Subunit compensation and plasticity of synaptic $GABA_A$ receptors induced by ethanol in α4 subunit knockout mice. *Front Neurosci* **5**:110.

Tretter V, Ehya N, Fuchs K, and Sieghart W (1997) Stoichiometry and assembly of a recombinant $GABA_A$ receptor subtype. *J Neurosci* **17**:2728–2737.

Tretter V, Jacob TC, Mukherjee J, Fritschy JM, Pangalos MN, and Moss SJ (2008) The clustering of $GABA_A$ receptor subtypes at inhibitory synapses is facilitated via the direct binding of receptor alpha 2 subunits to gephyrin. *J Neurosci* **28**: 1356–1365.

Tyagarajan SK and Fritschy JM (2014) Gephyrin: a master regulator of neuronal function? *Nat Rev Neurosci* **15**:141–156.

Vicini S (1999) New perspectives in the functional role of $GABA_A$ channel heterogeneity. *Mol Neurobiol* **19**:97–110.

Wafford KA, Bain CJ, Whiting PJ, and Kemp JA (1993) Functional comparison of the role of gamma subunits in recombinant human $GABA_A$/benzodiazepine receptors. *Mol Pharmacol* **44**:437–442.

Wafford KA, Thompson SA, Thomas D, Sikela J, Wilcox AS, and Whiting PJ (1996) Functional characterization of human gamma aminobutyric acid A receptors containing the alpha 4 subunit. *Mol Pharmacol* **50**:670–678.

Wallner M, Hanchar HJ, and Olsen RW (2003) Ethanol enhances alpha 4 beta 3 delta and alpha 6 beta 3 delta gamma-aminobutyric acid type A receptors at low concentrations known to affect humans. *Proc Natl Acad Sci USA* **100**: 15218–15223.

Weiner JL and Valenzuela CF (2006) Ethanol modulation of GABAergic transmission: the view from the slice. *Pharmacol Ther* **111**:533–554.

Whiting PJ, Bonnert TP, McKernan RM, Farrar S, Le Bourdellès B, Heavens RP, Smith DW, Hewson L, Rigby MR, Sirinathsinghji DJ, et al. (1999) Molecular and functional diversity of the expanding GABA-$_A$ receptor gene family. *Ann N Y Acad Sci* **868**:645–653.

Zezula J, Fuchs K, and Sieghart W (1991) Separation of alpha 1, alpha 2 and alpha 3 subunits of the $GABA_A$-benzodiazepine receptor complex by immunoaffinity chromatography. *Brain Res* **563**:325–328.

Address correspondence to: A. Kerstin Lindemeyer (Biochemistry), Department of Molecular and Medical Pharmacology, David Geffen School of Medicine at UCLA, Room CHS 23-338, 650 Charles E. Young Dr. South, Los Angeles, CA 90095-1735. E-mail: AKLindemeyer@mednet.ucla.edu or Jing Liang (Electrophysiology and Behavior), School of Pharmacy, University of Southern California, 1985 Zonal Ave. PSC 500, Los Angeles, CA 90089-9121. E-mail: lian743@usc.edu